GCOS Reference Upper-Air Network

GRUAN Technical Document

Review of Multiple-payload Radiosonde Sounding Configurations for Determining Best-Practice Guidance for GRUAN Sites

Hannu Jauhiainen, Masatomo Fujiwara, Rolf Philipona, Ruud Dirksen, Dale F. Hurst, Rigel Kivi, Holger Vömel, Belay Demoz, Nobuhiko Kizu, Tim Oakley, Kensaku Shimizu, Marion Maturilli, Thierry Leblanc, Fabio Madonna, and Richard Querel

Publisher
GRUAN Lead Centre

Number & Version
GRUAN-TD-7
Rev 1.0 (2019-01-25)

Document info

Title:	*Review of Multiple-payload Radiosonde Sounding Configurations for Determining Best-Practice Guidance for GRUAN Sites*
Topic:	Procedures
Authors:	Hannu Jauhiainen, Masatomo Fujiwara, Rolf Philipona, Ruud Dirksen, Dale F. Hurst, Rigel Kivi, Holger Vömel, Belay Demoz, Nobuhiko Kizu, Tim Oakley, Kensaku Shimizu, Marion Maturilli, Thierry Leblanc, Fabio Madonna, and Richard Querel
Publisher:	GRUAN Lead Centre, DWD
Document type:	Technical Document
Document number:	GRUAN-TD-7
Page count:	44
Version:	Rev 1.0 (2019-01-25)

Abstract

Various rigging configurations for multiple-payload radiosonde soundings have been used when characterizing different radiosonde instruments, when changing the radiosonde model at operational radiosonde sites or when flying specially developed scientific sensors together with a radiosonde. This paper describes such rigging configurations currently in use at sites of the Global Climate Observing System (GCOS) Reference Upper Air Network (GRUAN) or having been used during recent international radiosonde intercomparison campaigns. The advantages and potential issues for each configuration are discussed in detail. Though it is difficult to provide one single recommendation for all conditions, the paper aims at providing all the key information relevant to the multiple-payload configurations towards the future determination of the best-practice guidance for GRUAN and other sites.

Revision history

Version	Author / Editor	Description
Rev 1.0 (2019-01-25)	Hannu Jauhiainen, Masatomo Fujiwara, Rolf Philipona, Ruud Dirksen, Dale F. Hurst, Rigel Kivi, Holger Vömel, Belay Demoz, Nobuhiko Kizu, Tim Oakley, Kensaku Shimizu, Marion Maturilli, Thierry Leblanc, Fabio Madonna, and Richard Querel	First published version as GRUAN Technical Document 7 (GRUAN-TD-7)

Table of Contents

1 Introduction

The Global Climate Observing System (GCOS) Reference Upper Air Network (GRUAN) was established in 2008 to provide long-term, high-quality climate data records from the surface, through the troposphere, and into the stratosphere by using radiosonde and ground-based remote sensing instruments (*Seidel et al.*, 2009; *GCOS*, 2013; *Bodeker et al.*, 2016). The primary meteorological variables considered in GRUAN include temperature, water vapor concentration or relative humidity, pressure, horizontal wind, and geopotential height. In order for the data to be of sufficient value for probing climate trends, the characterization and validation of measurement uncertainties are the primary requirements (*Immler et al.*, 2010; *Dirksen et al.*, 2014), but long-term availability of the instruments is also an important factor. Ideally, inhomogeneities of the records due to any instrumental changes need to be avoided. However, technological advancement and instrumental development are always ongoing, and the instruments are manufactured with the aim to lead to smaller measurement uncertainty and to easier operation. All observation sites regularly undergo modernizations, where new instrument models are introduced and old models are put out of use. The only way to overcome this rather contradictory situation of wanting to be conservative and at the same time to aim for the best possible measurement data is that, at the time of instrumental changes, the differences in measurement between old and new models are quantified as accurately and extensively as possible. For the case of the radiosonde, it is essential to make sufficient intercomparison flights with the old and new instruments during the transition periods (*Kobayashi et al.*, 2012; *Jensen et al.*, 2016). One method for the intercomparison of two radiosonde models is to launch them on two separate weather balloons at the same time and from the same location, as this is the best representation of the standard operations expected by the radiosonde manufacturers. The challenge in this arrangement is that the two radiosondes typically follow different flight paths, both horizontally and vertically, through the atmosphere and sample different air parcels, affecting the interpretation of the results. A greater number of flights would therefore be needed to obtain statistically significant results about the differences in the measurements of the two radiosonde models. The actual number needed depends in part on random errors of the particular radiosonde type. Alternatively, two radiosondes can be connected to a single balloon to perform time-synchronized and co-located measurements. With this multiple-payload arrangement, all the sensors would measure essentially the same air parcel, making the uncertainty term related to the spatial and temporal differences negligible and thus making the number of flights required to obtain firm conclusions smaller. Multiple-payload arrangements are usually used during the instrumental transition periods at operational sites (*Kobayashi et al.*, 2012; *Jensen et al.*, 2016) and have been also used in the past international radiosonde intercomparison campaigns coordinated by the World Meteorological Organization (WMO) where more than two (typically four to six) radiosonde models were flown with a single balloon (*Nash et al.* (2011); see *Nash* (2015); *Jeannet et al.* (2008) and the references therein for all other WMO intercomparison campaigns). In general, the latest methods used in the WMO radiosonde intercomparison campaign (*Nash et al.*, 2011) would be considered good when similar combinations of instruments are to be flown. This multiple payload arrangement is also used to evaluate the reproducibility of a single radiosonde model by flying two identical models and to compare and validate an operational radiosonde model with an instrument whose measurement uncertainty has been well understood and quantified (*Fujiwara et al.*, 2003; *Vömel et al.*, 2007b; *Nash et al.*, 2011). Figure 1 shows a typical example of a multiple-payload rigging arrangement using booms and additional strings to attach several instruments to a single balloon.

There are several variations of multiple-payload rigging configurations described below, for which the advantages and disadvantages need to be evaluated. This applies to the way the various sondes are

Figure 1: Example of multiple-payload rigging arrangement at Lindenberg, Germany during the Lindenberg Upper-Air Method Intercomparison (LUAMI) during 3–24 November 2008. Operational radiosondes and scientific instruments are connected by booms and additional strings, and the whole payload is attached to a single weather balloon by the main string with a red parachute inline.

attached to the rig, which can have consequences for temperature and humidity measurements due to contamination, interference etc. The configuration needs to be chosen carefully so that the difference in the data uncertainty from that for a single-payload flight would be minimized. Major factors that need to be taken into consideration are e.g.

- Additional booms and strings may become a source of heat and water vapor contamination by wake effects (*Luers and Eskridge*, 1998; *Shimizu and Hasebe*, 2010). The characteristics of the material for the booms, e.g. weight, diameter, and surface hygroscopic and radiative properties, need to be considered.

- The pendulum and rotational motions of the payload relative to the balloon may become significantly different from what the manufacturers software filtering assumes for heat pulses, pendulum-motion component on wind measurements, etc (*Kräuchi et al.*, 2016).

- In reality, the choice may be limited by the weights and shapes of the instruments that are flown together.

At the 3rd GRUAN Implementation and Coordination Meeting (ICM-3) in Queenstown, New Zealand during 28 February – 4 March 2011 (*GCOS*, 2011), it was agreed that the GRUAN Task Team on Radiosondes would develop a best-practice guidance for multiple-payload configurations based on existing experiences. In this paper, information on multiple-payload configurations currently used at the GRUAN sites and during other activities, is summarized, particular, for the previous WMO radiosonde intercomparison campaigns (e.g. *Nash et al.*, 2011). Section 2 discusses physical effects influencing radiosonde temperature and humidity measurements. For identifying and determining the related uncertainty components, a brief review is performed on physical effects reported in the literature influencing the temperature and water vapor measurements. There exists a limited number of studies related to the balloon wake properties and instrument body effects on the temperature measurement. Section 3 describes several archetypes of assembly with balloon, parachute, main string, booms, additional strings, and radiosonde instruments, and discusses their possible effects on the measurement quality.Section 4 presents various multiple-payload configurations used at the GRUAN sites and during the past WMO radiosonde intercomparison campaigns. Section 5 presents various configurations for recent Vaisala RS92 and RS41 radiosonde intercomparison flights at GRUAN and other sites. Finally, in Section 6, discussions are made towards a future determination of the best-practice guidance for balloon payload configurations at GRUAN and other sites.

2 Physical Effects Influencing Temperature and Humidity Measurements

2.1 Temperature

Heat transfer mechanisms affecting radiosonde temperature measurements include thermal convection by air, shortwave and longwave radiation, and conduction from the sensor support structure (*Daniels*, 1968; *Luers*, 1990). In the ideal case the dominant heat exchange mechanism for in situ temperature measurements is convection and it is assumed that the sensor is always in thermal equilibrium with the ambient air. In reality this is not the case. At higher altitudes, where air density is low, the convection efficiency is accordingly small, and the other, heat exchange processes have a larger effect. In particular, daytime solar radiative heating can cause warm biases in temperature measurements of up to a few degrees at 10 hPa (*Nash et al.*, 2011). The magnitude of the biases depends in a complicated way on the radiative absorption and emission properties of the sensor coating as well as the sensor size, geometry, mechanical construction, and supporting structure. In general, a smaller sensor with a higher shortwave reflectivity has a smaller bias due to reduced solar radiative heating. Additionally, the sensor longwave emissivity should be low to minimize infrared cooling (*Schmidlin et al.*, 1986; *Luers*, 1990; *McMillin et al.*, 1992). Even for sensors that are specifically developed for upper-air temperature measurements, the bias errors caused by radiative processes must be compensated for in the data processing software (*Nash et al.*, 2011). This is usually performed by subtracting the estimated radiative effects from the raw measurements. The effects are estimated based on the radiosondes location in the atmosphere, solar elevation angle, and the assumed surface/cloud albedo below. There exist other methods to correct the radiative bias, e.g. an ”in-situ correction” method by using multiple sensors with coatings of different radiative properties (*Schmidlin et al.*, 1986; *Nash et al.*, 2011) and a method where the sensor is periodically shaded from the sun (*Philipona et al.*, 2013). Multiple-payload rigging for radiosonde soundings may cause additional bias errors for the temperature measurements through radiative and other processes. In the following such physical processes are discussed.

2.1.1 Shortwave and Longwave Radiation Effects

The amount of shortwave radiation affecting a temperature sensor in a multiple-instrument payload depends on the assembly configuration including the relative location of the booms if they are used. The shortwave radiation may be reduced by shadowing effects of nearby materials, or on the other hand may be increased due to reflection from nearby surfaces. For the latter case, the reflective properties of the nearby surfaces e.g. of other instruments, including the color and smoothness, are important factors. On the other hand, the amount of longwave radiation varies substantially depending on the direction the sensor is facing. Also, depending on the sensor properties (e.g. coating material), the sensor may have very different amounts of heat exchange either with clear sky (or space), or with low-level clouds, or even with surfaces of the nearby instruments, being at very different radiative temperatures (see e.g. *CIMO* (2014), Part I, Chapters 12.4.6 and 12.4.7). Rotation and pendulum motions of the payload usually reduce radiative errors because they tend to average out both shortwave and longwave radiation effects.

2.1.2 Wake From Nearby Structures

There will be temperature measurement biases if the measured air has been in contact with the balloon, parachute, booms, or other parts of the payload, with different temperatures from the ambient air. All surfaces are heated by daytime solar radiation and cooled, at night, by infrared radiation to space. In addition, the balloon gas is cooled by adiabatic expansion during ascent, cooling the balloon surface (see Section 3.1.1 for more details of the balloon wake issue). Careful payload assembly, including the use of sufficiently long suspension strings, is necessary (as quantitatively described in the next sections).

2.1.3 Effects Due to Reduced Ventilation

Multiple-payload rigging may affect the convective ventilation around the temperature sensor in various ways. Convection around the sensor generally decreases with altitude. The basic ventilation of the payload depends on the balloon ascent rate, which should be between 300 and 400 $m \cdot min^{-1}$ (i.e. 5 to 6.7 $m \cdot s^{-1}$) (Part II, Chapter 10 *CIMO*, 2014). In addition, horizontal movement of the payload relative to the ambient air, caused by the pendulum motion, adds to the ventilation. The speed of pendulum motion depends on the length of the main string and is influenced by the air resistance of the payload (e.g. the air resistance would be large if the parachute is placed near the payload). Also, nearby structures, e.g. the booms and other instruments may have effects on the ventilation. Other possible, probably minor, effects on the ventilation include the instruments rotational movement over its vertical axis and sensors small vibration in turbulent layers.

2.2 Humidity

Measurements of relative humidity require accurate, simultaneous temperature measurements of both the ambient air and the humidity sensor. The following rigging-related mechanisms related to water vapor measurement can be identified.

2.2.1 Moisture Emission from Surfaces or Materials of the Payload

While flying through moist layers, especially in the lower part of the atmosphere, the balloon, parachute, string, boom, instrument package, and other parts may collect moisture on their surfaces, or may even absorb it into their structures. The collected moisture may evaporate at higher altitudes, causing wet biases in the measurements when the water sensor is in the path of the shed moisture. This contamination can be easily detected by instruments with sensitivities high enough to measure the low levels of stratospheric humidity (*Vömel et al.*, 2007a). Water vapor measurements using the NOAA Frost Point Hygrometer (FPH) have been made during controlled balloon descent to minimize the contamination problem (*Hurst et al.*, 2011; *Kräuchi et al.*, 2016). Direct comparisons of the ascent and descent moisture profiles can identify ascent measurements affected by contamination in the stratosphere. Upper tropospheric relative humidity measurements using operational radiosondes can also be affected by contamination problems and, in the lower troposphere, by the freezing of super-cooled droplets, collected on the humidity sensor itself. As an example to reduce these problems, each Vaisala RS92 radiosonde is equipped with two sensors that are alternately used for the measurement or heated to remove contamination (*Verver et al.*, 2006; *Nash et al.*, 2011).

2.2.2 Effects on Humidity Sensor Temperature

For radiosonde measurements, relative humidity is measured with respect to the temperature of the humidity sensor, which can be different from the ambient air temperature. All previously discussed rigging-originated effects that interfere with the temperature measurements may also affect the temperature of the humidity sensor. For relative humidity sensors that do not have their own temperature sensor (see *Nash et al.* (2011)), Annex D, Table D4.1), the sensor temperature is often assumed to be equal to the measured ambient temperature. Therefore, if the humidity sensor temperature is higher than the ambient temperature due to, e.g. solar radiative heating, the relative humidity reading would be lower, causing a dry bias in the measurements (*Vömel et al.*, 2007c).

3 Configuration of a Multiple-payload System

The components of the multiple-payload system typically include a balloon, parachute, main string, and payload. The assembly of the payload may have several kinds of implementations for instruments including supporting booms and additional strings. An unwinder/de-reeler (Figure 2) may be used to increase the distance between the balloon and payload after launch and to ensure successful and smooth deployment. Figure 3 presents the typical components of the multiple-payload system, as will be referred to later in this paper.

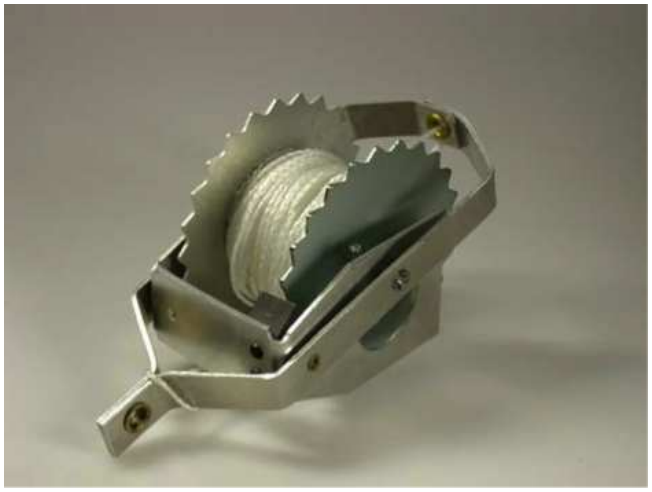

Figure 2: An example string unwinder (GRAWs model UW1 series). The string is 0.8 mm in diameter, with either 30 m (UW1-30) or 50 m (UW1-50) length. The maximum mass of the payload that can be held is 5 kg. Once launched, the unwinding speed is $0.1\,m \cdot s^{-1}$ for a 210 g payload and $0.3\,m \cdot s^{-1}$ for a 2.5 kg payload.

3.1 Balloon and Main String

Usually, larger-size rubber or plastic balloons (1200 – 3000 g) are used to obtain the ascent rate of 300 to $400\,m \cdot min^{-1}$ (*CIMO*, 2014) and appropriate balloon-burst altitudes. The balloon may affect the measurements by its thermal wake and by moisture shedding, in combination with the pendulum, rotational and other anomalous motions of the payload. If the payload is very close to the balloon, the ventilation of the sensors may also be affected by turbulence produced near the balloon. Therefore, a long string (e.g. 30 m or 60 m or even longer, depending on the purpose) is usually used, and highly recommended, to separate the payload from the balloon in flight (Part I, Section 12.7.4 *CIMO*, 2014).

3.1.1 Balloon Wake

There are some studies on the balloon thermal wake. *Tiefenau and Gebbeken* (1989) made a theoretical analysis to calculate the daytime-heating and nighttime-cooling effects caused by meteorological balloons. During nighttime ascents, the adiabatic heat loss within the balloon lowers the internal gas and balloon skin temperature by $\sim$10 K or more. During daytime ascents, solar radiation heats the balloon skin, superimposing a heating effect upon the adiabatic cooling effect on the balloon skin. The resulting skin temperature of the balloon affects the airstream passing over the balloon via heat

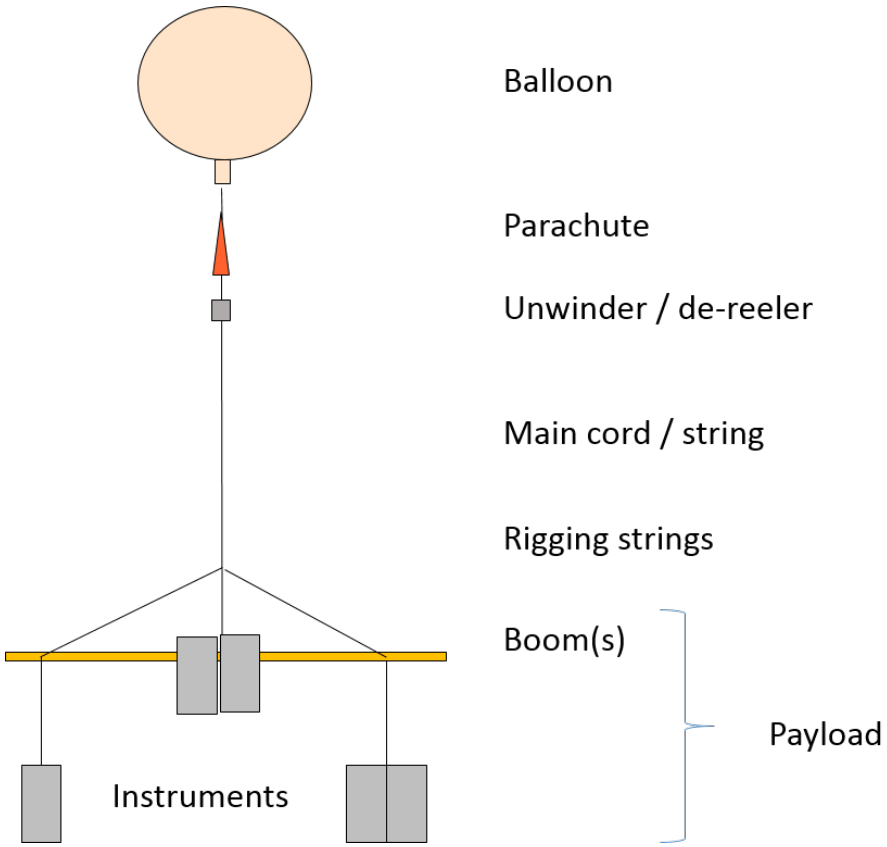

Figure 3: A schematic example of a multiple-payload system presenting the components, i.e., balloon, parachute, unwinder/de-reeler, main cord/string, rigging strings, boom(s), and instruments. A group of boom(s), instruments, and connecting strings is called payload.

exchange. *Jumper et al.* (2003) studied the dependency of balloon wake effect on string length using optical turbulence measurements. Though definitive quantification was not possible, the observed tendency was for payloads to encounter more wake:

1. when shorter string lengths were used;
2. at higher altitudes when the balloon has its largest diameter; and
3. in lower wind shear conditions.

Another tendency was that tropospheric wake encounters result in smaller thermal perturbations than those in the stratosphere due to the smaller temperature differences between the ambient air and the balloon skin (perhaps due to less convective heat transfer in the stratosphere). *Shimizu and Hasebe* (2010) measured the balloon-surface and balloon-gas temperatures and found that at 30 km, the balloon surface was ∼20 K warmer than the ambient air during daytime and ∼5 K colder than the ambient air during nighttime. Furthermore, they marked that because the sensor on the balloon surface was located in an area that was less exposed to solar radiation, the temperature of the balloons top part must have been at a much higher temperature during the daytime. They also showed that in case of a short suspension string (15 m in this case) it is possible to detect the balloon wake effects with a fast-response temperature sensor).

3.1.2 Main String and Unwinder

A string is used to connect the payload to the balloon and to keep a sufficient distance between the two elements for the measurement purpose. The typical material for this string includes cotton and polypropylene. The length of the string in operational soundings varies from 10 to 60 m. In research and test purposes, especially when larger-size balloons are used, longer main strings are generally favored. The purpose of this string is to avoid the case where the sensors are flying for long periods of time within the balloon wake. On the other hand, a very long string may complicate the balloon launch procedure particularly under windy conditions. To make the balloon-payload system compact at the launch, an unwinder/de-reeler (Figure 2) is often used. The unwinders extend the string length immediately after launch, typically taking a few minutes to full extension, by use of the force between the balloons buoyancy and the payloads gravity. Sometimes, the unwinder may get jammed which often results in the suspension being too short.

3.2 Parachute

A parachute is used particularly for a heavy payload to reduce the descending speed after the balloon burst (ideally down to $\sim 5\, m \cdot s^{-1}$ near the surface), thereby minimizing the probability of accidents when the payload reaches the ground. There are several types (size and shape) of parachutes. The parachute may be connected directly to the balloons neck, or may be connected to the balloon with e.g. $\sim$1 m length string. The latter is to avoid the case where after the balloon - bursts, balloon-material pieces cause the parachute to malfunction. There is also a method where the parachute is contained within the balloon, an option which is primarily used for automatic launch systems but have also been used successfully in intercomparisons in an attempt to maximise the balloon burst heights by minimizing the drag caused by the parachute. During ascent the parachute may cause heat and moisture contamination similar to that of the balloon. The size and type of the parachute, as well as its location in the flight train, affects the pendulum motion and sensor ventilation. To minimize the potential influences on the measurements, it is beneficial to place the parachute (and other components such as a radar reflector for the radar tracking system) close to the balloon at a separation ensuring good parachute operation.

3.3 Assembly of the Multiple Payload

When choosing particular rigging boom(s) to separate the instruments for a multiple-payload flight, the following major points need to be considered. First, the boom(s) should be strong enough to withstand any sudden, strong forces during launch and in turbulent layers during flight. Second, for air traffic safety the density of the boom material should be such that it will disintegrate (e.g. on impact with an aircraft fuselage or propeller and ingestion by a jet engine). Finally, the surface properties (e.g. reflectivity and hygroscopy) of the boom should minimize influences on the measurements. Commonly used materials for rigid or hollow booms include wood, bamboo, plastic, carbon fibre, and expanded polystyrene. In commonly used multiple-payload configurations, the instruments are either hung below a boom with a short string, or are firmly attached to it with the sensors positioned well above the boom. For the former case, it should be noted that the boom may produce thermal wake and moisture emission like balloons do. In daytime conditions, solar radiative heating raises the temperature of the boom, particularly at higher altitudes, while during night, infrared cooling lowers the temperature, depending on the surface radiative properties. To prevent daytime heating, it is beneficial to use material with high shortwave reflectivity (e.g. light colored, glossy). Because the

width of the wake depends on the dimensions of the boom, it is advantageous to use a smaller diameter boom, keeping a sufficient strength as noted above. To minimize the moisture contamination it is beneficial to use a material whose surface is hydrophobic. On the other hand, when the instruments are firmly attached to the boom, the dimensions of the boom and the relative positions of the boom and sensors are important. A large boom positioned very close to or even partly above the sensors may affect the sensor ventilation and contaminate the temperature/humidity measurements. For this reason, it is advantageous to use a smaller boom with good radiative and hygroscopic properties. It should be noted that for sensors that have direction-dependent radiative properties (e.g., temperature sensors with direction-dependent solar reflectivity for daytime soundings), fixing the instrument to the boom may produce measurement biases because the sensors rotation relative to the sun may be much slower than that for a single-payload sounding (*von Rohden et al.*, 2016) see also Section 5 below. There are other important aspects to be considered for multiple-payload assemblies:

1. the solar radiation may be intensified by direct reflections from the boom or may be periodically attenuated by shadowing effects;
2. there are national and international regulations on the total mass of the payload; and
3. instruments operating in close proximity to radiosondes may not work properly due to radio frequency interference and must be moved farther away.
4. Health and Safety for the personnel involved in the launch.

4 Review of Various Multiple-Payload Configurations

In this section, several configurations for the multiple-payload radiosonde soundings are presented. Potential influences on the quality of temperature and humidity measurements are described, mostly from theoretical considerations, without actual flight tests and analysis of the probability or severity of the influences. Some configurations may produce measurement biases, while some may increase random measurement variability.

4.1 Single Radiosonde Sounding as a Reference

As a reference for the later sections, Figure 4 presents a configuration for a single radiosonde attached to a balloon. A parachute, unwinder, main string and radiosonde are fastened below the balloon. The aerodynamic properties of the setup depend on the detailed configuration. The key point for this assembly is the relatively free movement of the radiosonde. The radiosonde typically swings like a pendulum beneath the balloon with various modes of motion. If the main string is relatively long with a torsion, the radiosonde may have free rotation around the vertical axis. It is noted that any data processing software provided by a manufacturer, e.g. a low-pass filtering for wind and other variables, may assume a periodicity of the pendulum motion based on the particular configuration (e.g. the length of the main string/unwinder, no additional payload, etc.). It is thus recommended to check the assumptions used in the manufacturers software and to evaluate the impact on the data quality if a different flight configuration is applied.

4.2 Multiple Payload Without Booms

Figure 5 presents an example of a payload assembly where two or more instruments are directly attached together at the end of the main string without any booms. This enables a simple construction and an easy payload launch because of its compactness. Factors to be considered include the larger top cross section and volume of the instrument package, which may reduce ventilation of the sensors, collect more moisture, and cause more heat contamination compared to a single instrument flight. The combined package may also have radiative effects such as increased solar reflection or shadow effect that could significantly influence the temperature measurements. Due to the larger momentum of inertia and drag, the rotational motion of the payload around the main string may be slightly reduced.

4.3 Multiple Instruments Hanging on Booms

A common method to intercompare multiple radiosonde instruments is to hang them on a single boom or multiple booms. Figure 6 presents the schematic construction of a single boom with three radiosondes hanging below. Figure 7 presents an actual example of single boom setup being used in the field. A multiple-boom assembly makes it possible to fly several radiosondes, up to 6 or 8, with one 3 kg balloon, without them hitting each other. This configuration was used in the past WMO radiosonde intercomparison campaigns (see, Figure 3.1 and Annex C of *Nash et al.* (2006); Figures 2 and 4 of *Jeannet et al.* (2008); several photographs in *Nash et al.* (2011)). Figures 8 and 9 show a multiple-payload setup with three bamboo booms that accommodated six radiosondes during the 2010 WMO radiosonde intercomparison campaign at Yangjiang, China (*Nash et al.*, 2011). Figures 10 and 11 show a multiple-payload setup used during the 1993 WMO radiosonde comparison campaign at Tsukuba, Japan (*Yagi et al.*, 1996). Figure 12 shows the setup used during the 2001 WMO campaign at Alcântara, Brazil (*da Silveira et al.*, 2003).

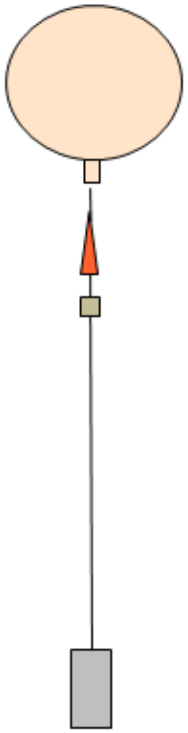

Figure 4: Schematic drawing of a single radiosonde payload attached to a balloon and a parachute through a main string including an unwinder. A typical length of the main string including an unwinder is 30 m to 60 m.

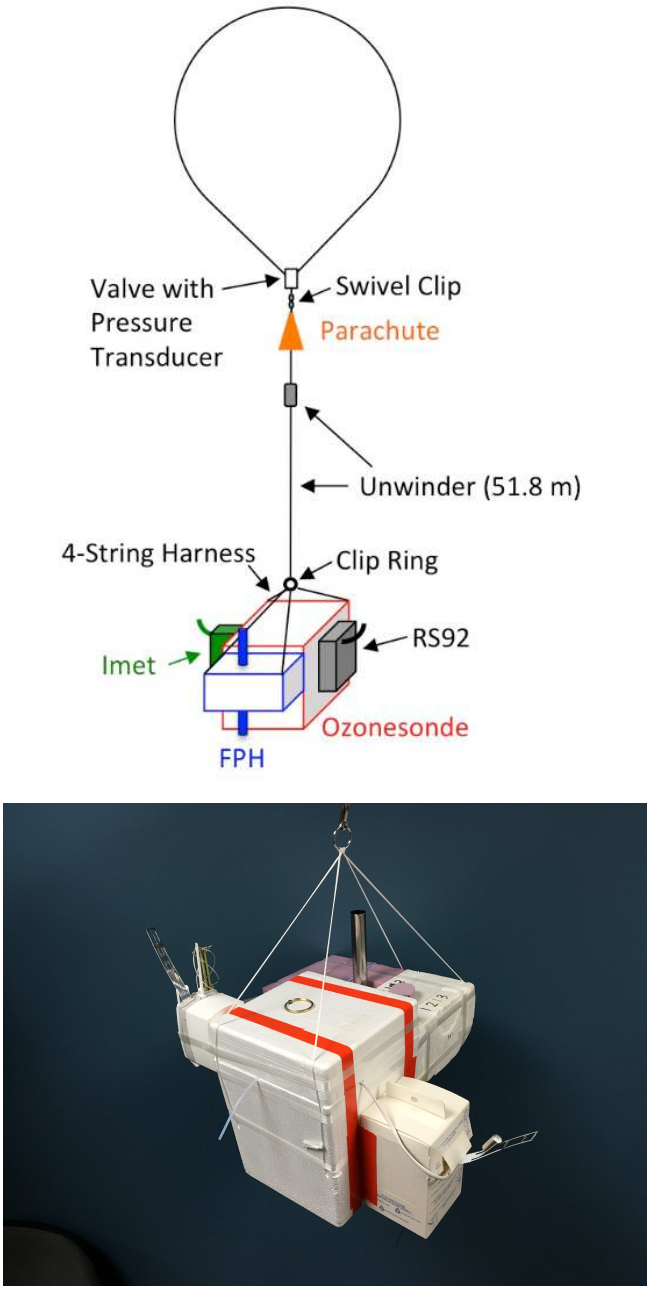

Figure 5: A schematic illustration (top) and a photograph (bottom) of a multiple payload example without booms. This configuration is used at Boulder (39.95°N, 105.20°W), Colorado, USA, and Lauder (45.04°S, 169.68°E), New Zealand for the long-term monitoring of upper atmospheric water vapor and ozone. The payload includes an InterMet iMet-1-RSB radiosonde, a NOAA Frost Point Hygrometer (FPH) for measurements of water vapor, an electrochemical concentration cell (ECC) ozonesonde for measurements of ozone, and a Vaisala RS92 radiosonde. A valve system inserted into the balloons neck slowly releases helium gas from the balloon at a pre-set pressure in the stratosphere, producing a controlled descent at rates of 4-6 $m \cdot s^{-1}$ to obtain stratospheric water vapor data with minimum contamination due to outgassing (*Kräuchi et al.*, 2016).

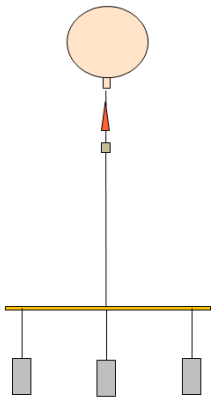

Figure 6: Schematic drawing of three radiosonde instruments hanging from a single boom.

Figure 7: An example of multiple instruments hanging from a 2 meter-long boom of solid cylindrical Styrofoam. Taken at the Howard University-Beltsville site (39.05°N, 76.88°W), Washington, D.C., USA. The same boom is also used by the National Weather Service Sterling Field Support Center (SFSC) for multi-payload operations.

Figure 8: Preparation of a multiple-payload assembly using three bamboo booms during the 2010 WMO radiosonde intercomparison campaign at Yangjiang (21.83°N, 111.97°E), China. The ∼3 m-long bamboo booms were temporarily situated on top of the aluminum-frame holder during preparation. A string of ∼0.7 m length was used to hang each radiosonde from a boom (note that during the preparation period, shown in this photograph, each string was wound around the boom so that the instruments did not touch the ground).

Figure 9: Just after a launch of the multiple payload shown in Figure 8 during the 2010 WMO campaign at Yangjiang, China.

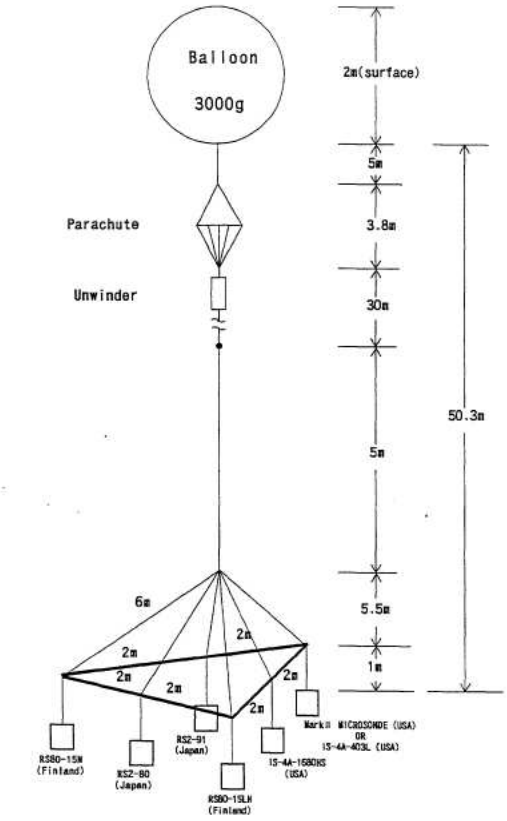

Figure 10: A schematic illustration of the multiple-payload assembly used during the 1993 WMO radiosonde comparison campaign at Tsukuba, Japan. Taken from *Yagi et al.* (1996).

Figure 11: Photograph showing a balloon launch during the 1993 WMO radiosonde comparison campaign at Tsukuba, Japan.

Figure 12: Photograph showing a boom with three radiosondes hanging, being prepared for balloon launch during the 2001 WMO radiosonde comparison campaign at Alcântara, Brazil.

Compared to the single-radiosonde flight, the booms may influence the temperature and humidity measurements (see Section 3). During the 2010 WMO campaign, the Meisei Temperature Reference (MTR) sonde, using an ultra-thin tungsten wire (*Shimizu and Hasebe*, 2010), detected heat pulses during daytime flights probably due to solar heating of the boom (*Nash et al.*, 2011). One more factor to be considered is that the pendulum and rotational motions of these various configurations of payloads probably differ significantly from one to another, and from those for the single-instrument flight case. This may influence the data quality if the data processing software (e.g. low-pass filtering) assumes specific pendulum and rotational motions as discussed in Section 4.1, and, therefore, affect the comparability of the datasets collected in different experiments.

4.4 Multiple Instruments Fixed to Booms

To prevent the booms from affecting the radiosondes hanging below, it is also possible to fix the radiosondes directly to the booms (Figures 13, 14, 15 and 16)
In this case, it is important to set the sensors so that the booms do not affect the measurements through their wake and/or radiation. It is also noted that as the momentum of the boom-instrument system becomes large, the rotational motion of the instruments is reduced compared to that of a single radiosonde or multiple radiosonde hung from a boom with strings. Again, reduced rotational motion may influence the data quality if the data processing software (e.g. low-pass filtering) assumes a specific rotational motion as discussed in Section 4.1.

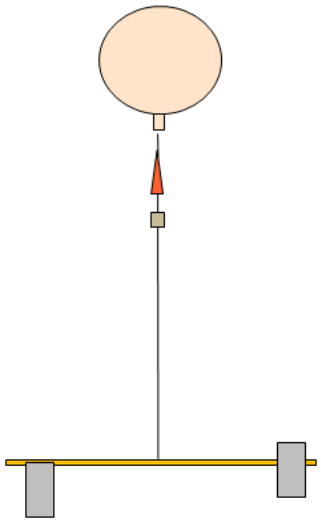

Figure 13: Schematic drawing of two instruments fixed to a boom.

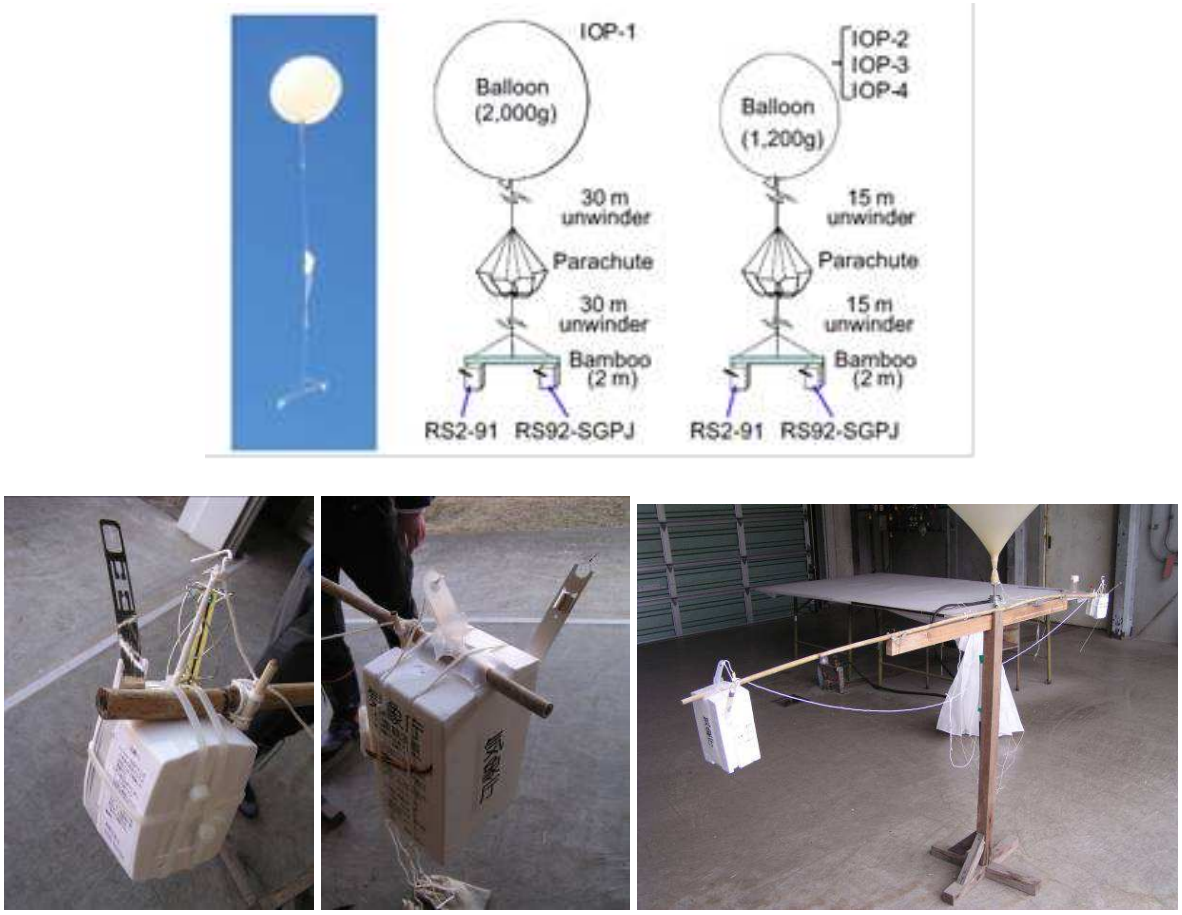

Figure 14: Schematic illustration for two different string lengths (top) and photographs of two radiosondes fixed to a boom (bottom) at Tateno (36.06°N, 140.13°E), Japan (see *Kobayashi et al.*, 2012). During the Intensive Observation Period (IOP) 1, in winter, a larger-size balloon (2000 g), with a longer (60 m in total) string, was used to reach higher altitudes. For all cases, Vaisala RS92 and Meisei RS2-91 radiosondes were attached to a 2 m-long bamboo boom.

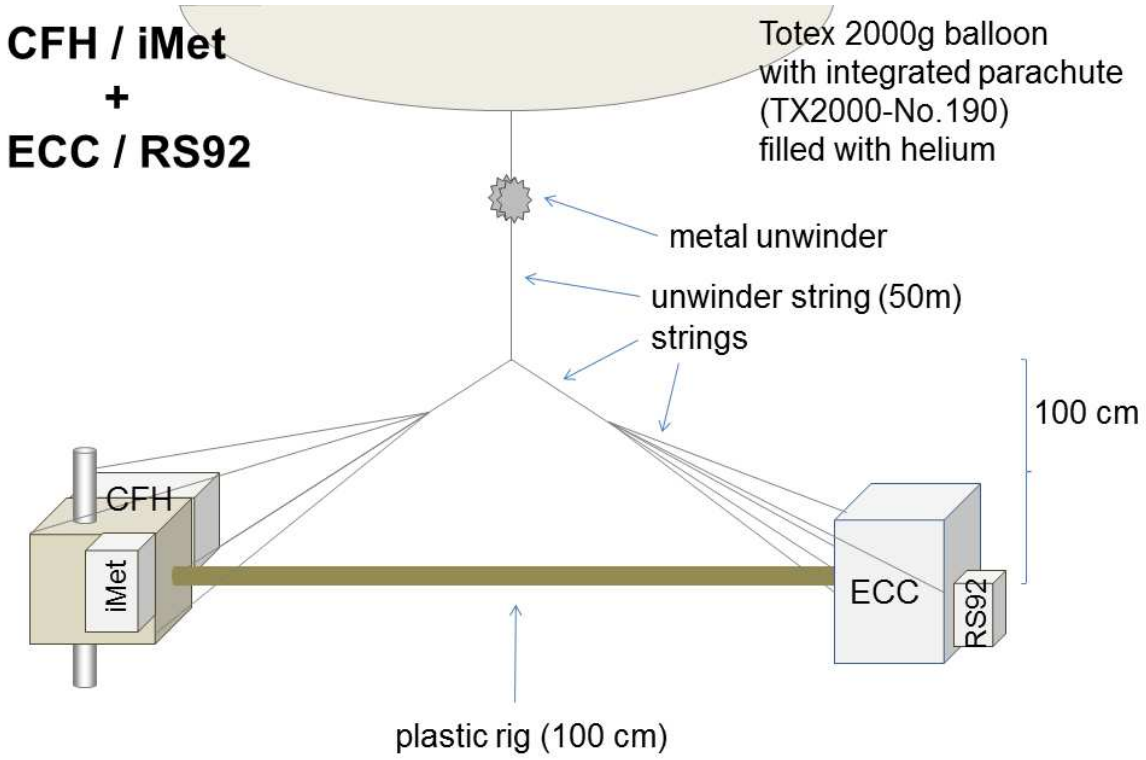

Figure 15: Schematic illustration of instruments fixed to a rod, used at Ny-Ålesund (78.92°N, 11.92°E), Svalbard, Norway, during the period September 2013 to January 2017. The CFH (Cryogenic Frostpoint Hygrometer) soundings are performed to detect the stratospheric water vapor distribution, and the according data are available via the Network for the Detection of Atmospheric Composition Change (NDACC).

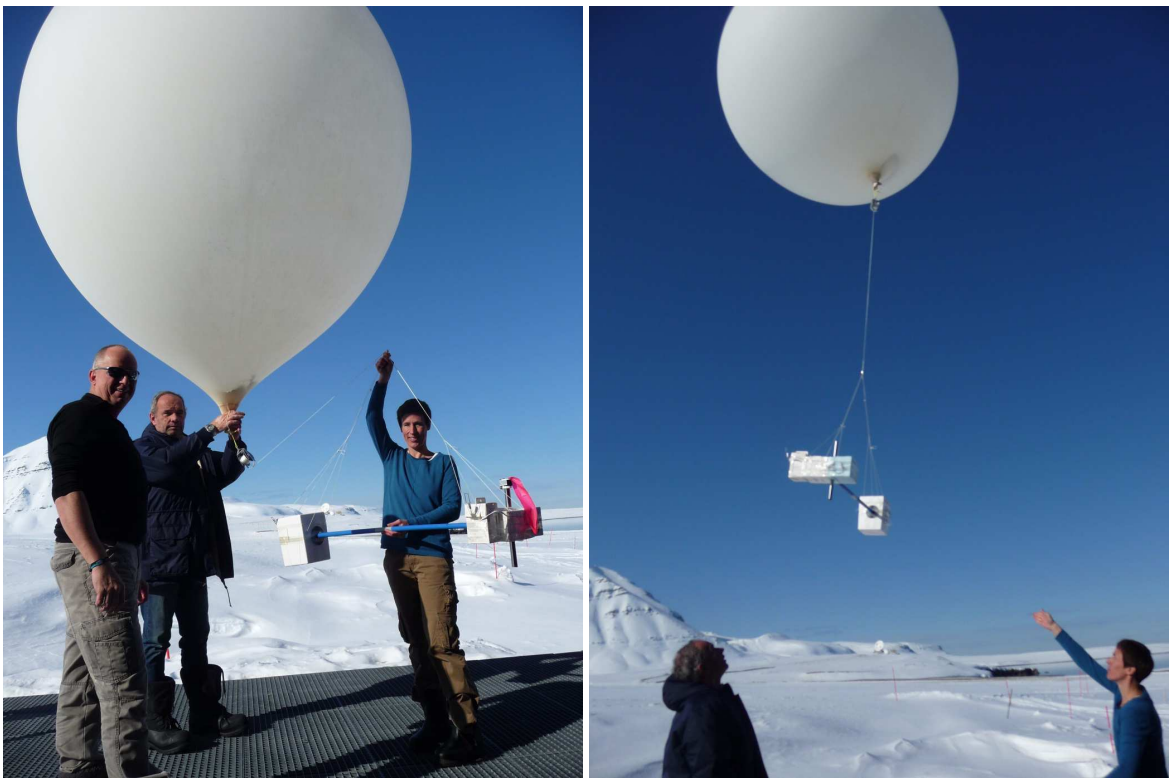

Figure 16: Photographs showing a sounding of an iMet radiosonde with CFH (Cryogenic Frostpoint Hygrometer), and a RS92 radiosonde with ECC ozonesonde fixed on a 1 m-long plastic rod, at Ny Ålesund (78.92°N, 11.92°E), Svalbard/Norway. The set-up was used in the period September 2013 to January 2017.

4.5 Multiple Instruments Attached to the String Vertically

Instruments can also be attached at different locations along the main string without using a boom (Figure 17). In this arrangement, it is important to keep the distance between the instruments large enough to prevent thermal or moisture wake influences on the instruments below. As the speed of pendulum movement increases with distance from the balloon, the ventilation efficiency of each instrument will depend on its location. For example, this would influence the results when comparing wind measurements of radiosondes at different locations along the string. This setup also guarantees that instruments are never at the same altitude simultaneously, so intercomparisons of their measurements require time synchronization based on the measured ascent rate of the balloon.

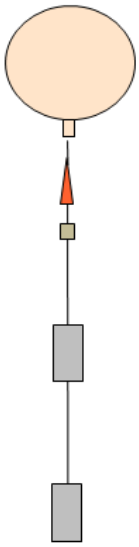

Figure 17: Schematic drawing of two instrument packages attached at different locations along the main string.

4.6 Combined Assembly

In addition to the basic multiple-payload assemblies presented above, a large number of variations are possible. Figure 18 presents a schematic drawing of one such configuration. Figures 19, 20, 21, and 22 shows actual examples of combined multiple payload assembly. Viewpoints to consider are the same as for the lighter ”archetype” assembly solutions presented above. However, a heavier payload and a more rigid fixing may enhance the effects discussed above.
‘

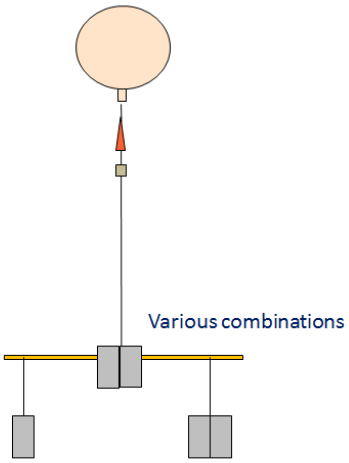

Figure 18: Schematic drawing of a combined assembly using a single boom.

Figure 19: An example of combined multiple-payload assembly during the 2010 WMO radiosonde intercomparison campaign at Yangjiang, China. Two ∼3 m-long bamboo booms were crossed. At the center, the Cryogenic Frostpoint Hygrometer (CFH) was situated on top of the booms. At the four boom ends, radiosonde instruments (including the Lockheed-Martin Sippicans LMS6 Multi-thermistor sonde (left) and the MTR sonde with Meisei RS-06G radiosonde (right, front)) were hung with ∼0.7 m string (part of this was wound around the boom during this preparation period). The bamboo booms were temporarily situated on top of the aluminum-frame holder during the preparation.

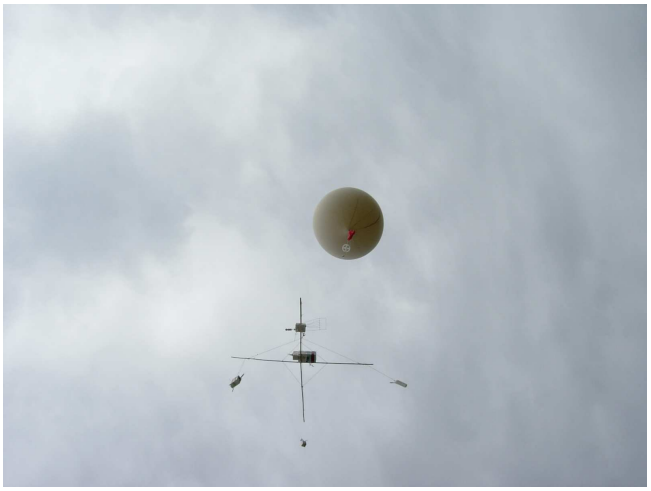

Figure 20: Just after the launch of the multiple payload shown in Figure 19 during the 2010 WMO campaign at Yangjiang, China.

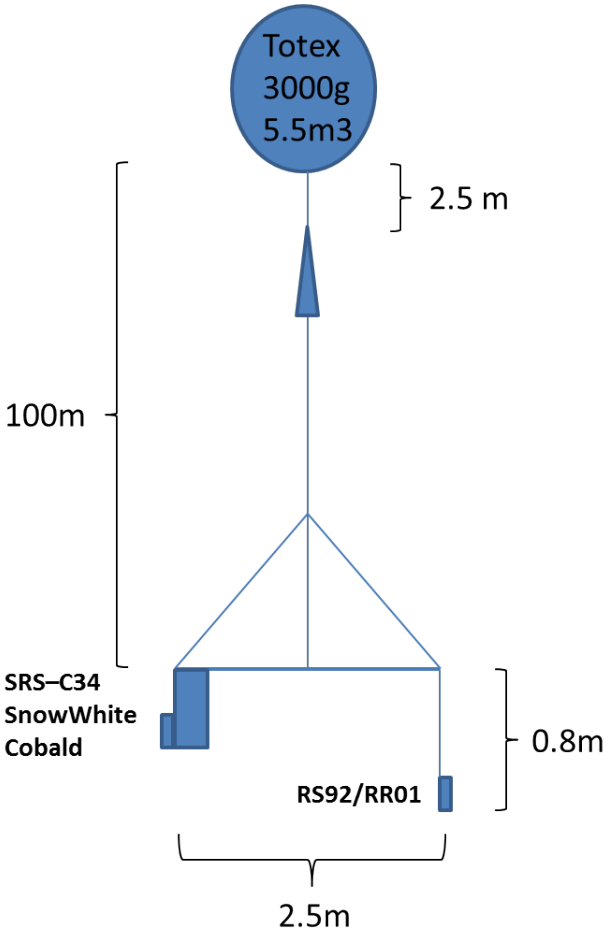

Figure 21: An example of the combined multiple payload assembly at Payerne (46.81°N, 6.95°E), Switzerland, used for all GRUAN comparison flights on a weekly basis. All comparison flights are performed with this configuration, only the radiosonde types attached under the bamboo rod can change. Used payloads were Meteolabor SRS-C34 radiosonde (linked with Snow-White frost point hygrometer and/or COBALD), SRS-C50, RS92, RR01 and RS41.

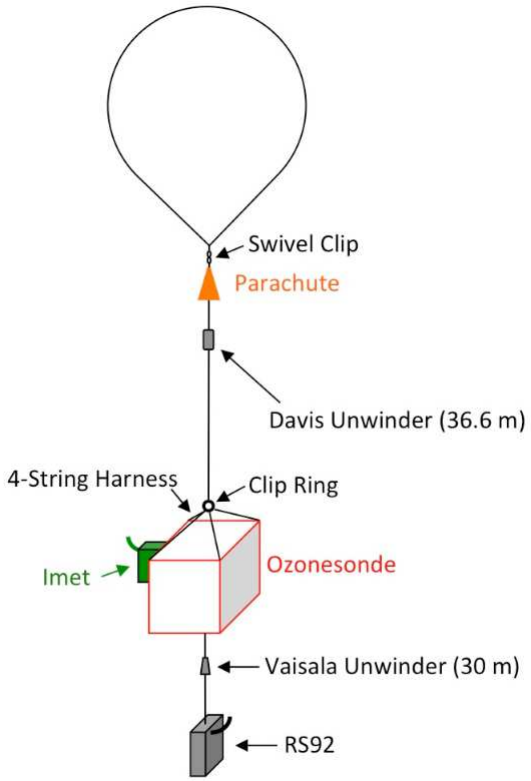

Figure 22: An example of combined assembly at Boulder, USA, using two unwinders. The first unwinder connects the balloon to an ECC ozonesonde and iMet-1-RSB radiosonde. A second unwinder situates the RS92 radiosonde 30 m below the main payload. This configuration is flown for the long-term monitoring of upper atmospheric ozone.

5 RS92-RS41 dual sounding flight configurations

In 2013, Vaisala released a new radiosonde RS41, the successor of the RS92. Shortly thereafter, several GRUAN and other sites started intercomparison flights of these two radiosondes. At the 8th GRUAN Implementation and Coordination Meeting (ICM-8) in 2016 at Boulder, USA, the participants agreed that the Task Team on Radiosondes would collect information on the RS92-RS41 dual sounding rig configurations from these intercomparison sites. In this section, the dual sounding rig configurations recommended by the GRUAN Lead Centre at Lindenberg, Germany, and by Vaisala are presented, and then those used at Camborne (UK), Lamont (Oklahoma, USA), Ny Ålesund (Svalbard, Norway), Lauder (New Zealand), Payerne (Switzerland), and Sodankylä (Finland) are reviewed.

5.1 GRUAN Lead Centre recommendation for RS41-RS92 dual soundings

Partly based on the results of RS92-RS41 dual soundings performed at Lindenberg using various configurations of the payload, *von Rohden et al.* (2016) gave a recommendation for the payload configuration for performing soundings with two radiosondes. A particular focus was placed on whether the radiosondes should be fixed to or hung from the boom. The conclusion is that hanging (see Figure 23) allows an independent irregular rotation of the sonde and, though the variance of the data is still dominated by radiative heating, it is expected to be "closer" to stochastic in nature. They also provided a typical rigging example for an extended payload including the two radiosondes, CFH, and ozonesonde.

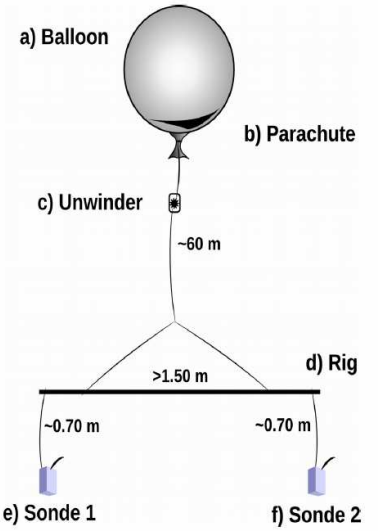

Figure 23: Recommended setup by the GRUAN Lead Centre. To prevent heat and water vapor contamination, a wooden rod (e.g., bamboo) is a good choice for the boom. Also, the distance from the balloon to the boom should be at least 60 m. The length of the boom may be $\geq$1.5 m, to avoid possible telemetry interferences and radiative interaction from the device housings as well as to ensure the clearance necessary for the free movements in case of hanging devices require a certain horizontal distance. Taken from *von Rohden et al.* (2016).

5.2 Vaisala recommendation for RS41-RS92 dual soundings

Recommendations from manufacturers are based on their experiments and experiences and thus should be the first choices if there are no other evidence-based recommendations. The following is Vaisalas recommendation for RS41-RS92 dual soundings (see also Figure 24). The key purpose of radiosonde intercomparisons is to understand differences in the behavior of radiosondes in operational use. To meet this target, it is important to ensure that the test setup does not introduce phenomena that are not present in the operational radiosoundings where radiosondes fly as single units. The most important aspects are: (1) Adequate ascent rate; and (2) the hanging of radiosondes from booms with 80 cm string. Proper ventilation of the radiosondes is essential for obtaining high quality data. To ensure proper ventilation a balloon ascent rate is at least $5\,m \cdot s^{-1}$ on the average. Remember also to adjust the lift according to local weather conditions. Heavy rain or high wind may require to increase balloon lift force in order maintain high enough balloon ascent rate. To minimize unwanted ventilation effects caused by the boom, use at least 80 cm long lengths of original radiosonde string to hang the radiosondes from the boom. Secure the connections with tape. The unwinder string length can vary but minimum shall be 30 m, 60 m is recommended. For safety reasons a parachute should always be used.

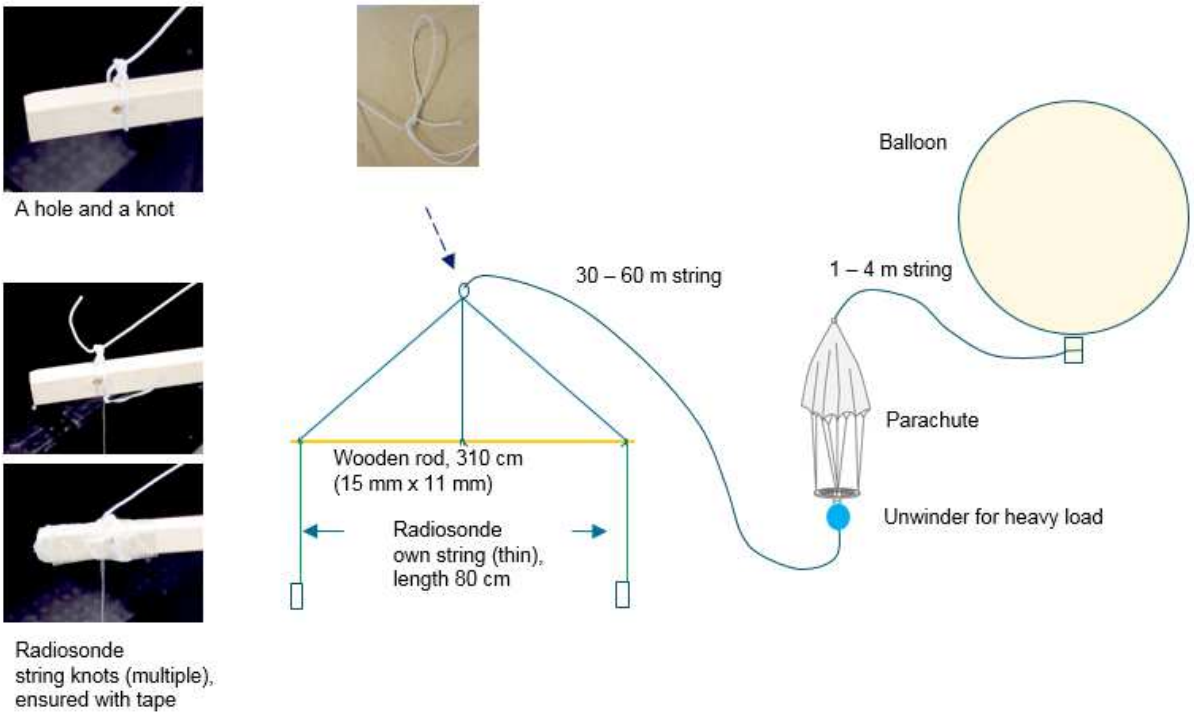

Figure 24: RS92-RS41 dual sounding rigging method recommended by Vaisala. Large size e.g. 1200 g meteorological weather balloon should be used for giving a nominal ascent rate of $5\,m \cdot s^{-1}$. The unwinder is connected directly to the parachute. The length of the main string is 50 m. Payload support strings are triangle-shaped to balance the wooden boom (3.1 m, 15 x 11 mm^2). Radiosondes are hung ∼80 cm below the boom with string taken from the Vaisala unwinder). All the connection points should be secured with a tape.

5.3 Camborne, UK (Met Office)

Edwards et al. (2014) reported the results of their RS92-RS41 intercomparison flights at Camborne (50.27°N, 5.33°W), UK during 7–19 November 2013. Figure 25 shows their method of rigging for two RS92 and two RS41 radiosondes.

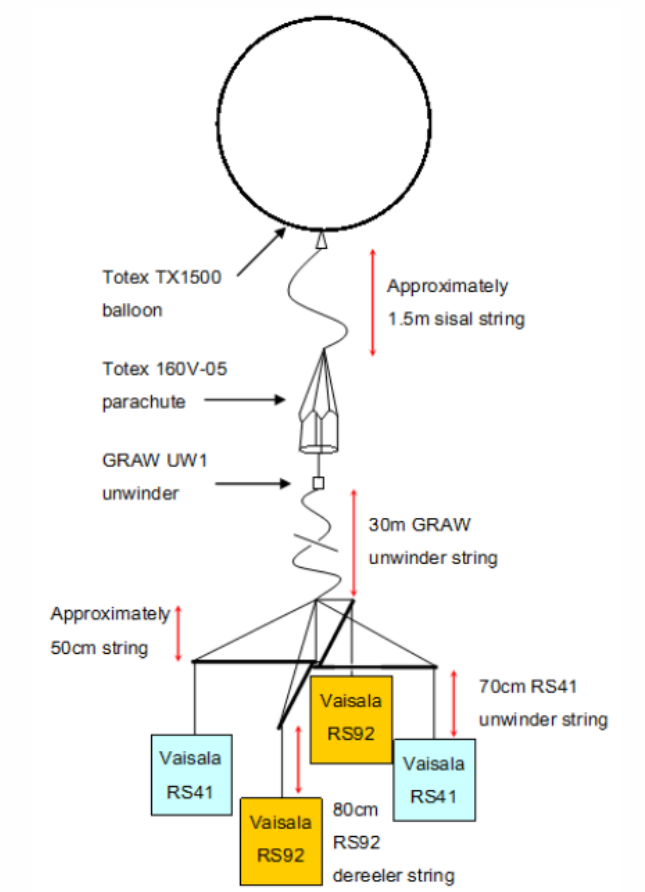

Figure 25: The multiple payload configuration of two Vaisala RS92 radiosondes and two Vaisala RS41 radiosondes used at Camborne, UK. Taken from *Edwards et al.* (2014).)

5.4 Lamont, Oklahoma, USA

Jensen et al. (2016) presented results of their RS92-RS41 comparison flights at the US Department of Energys Atmospheric Radiation Measurement (ARM *Mather and Voyles*, 2013) Southern Great Plains facility site near Lamont, Oklahoma (36.70°N, 97.49°W), USA during 3–8 June 2014. Figure 26 and 27 shows their method of rigging.

5.5 Lauder, New Zealand

Figure 28 show the setup used at Lauder, New Zealand.

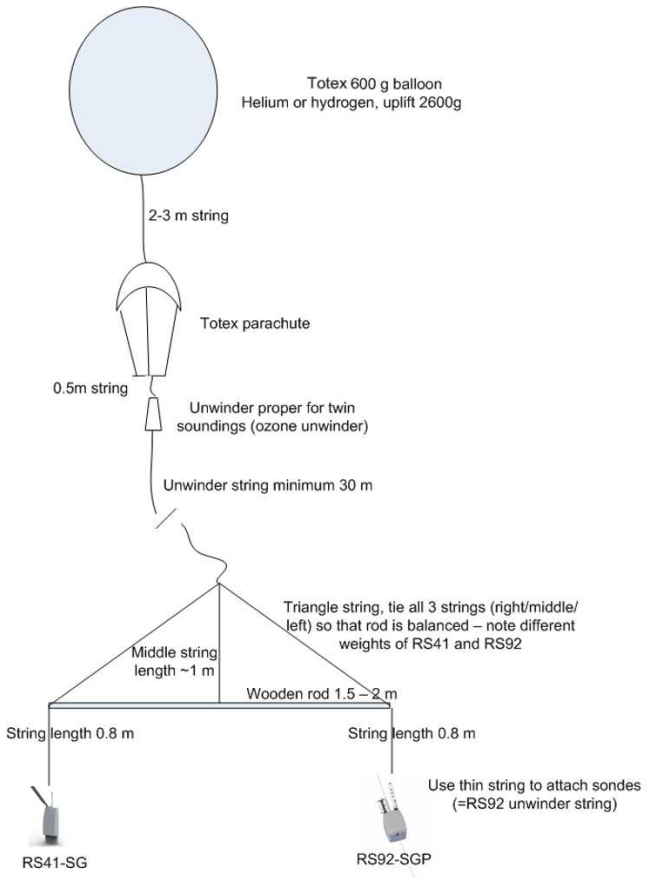

Figure 26: The experimental set-up for the RS41-RS92 dual soundings used at Lamont, Oklahoma, USA. Taken from *Jensen et al.* (2016).

5.6 Ny Ålesund, Svalbard, Norway

Figures 29 and 30 show the setup used at Ny Ålesund, Norway.

5.7 Payerne, Switzerland

Figure 31 shows the setup used at Payerne, Switzerland.

5.8 Sodankylä, Finland

Figure 32 shows the setup used at Sodankylä, Finland.

Figure 27: Photograph of a RS92-RS41 dual sounding at Lamont (*Jensen et al.*, 2016).

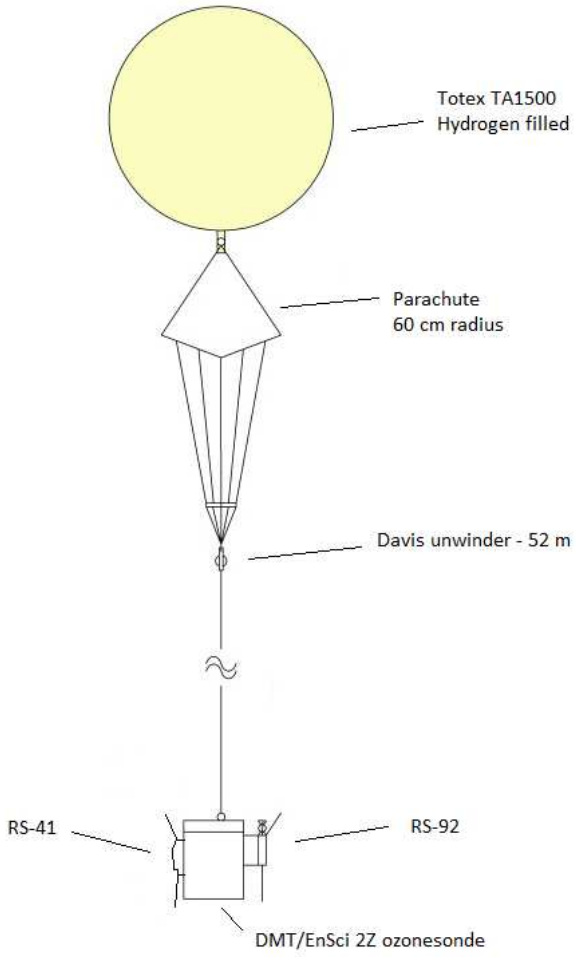

Figure 28: The configuration of the RS41-RS92 flights at Lauder, NIWAs Atmospheric Research Station in New Zealand. The RS92 and RS41 radiosondes are placed, sensor booms pointing outwards, on opposite sides of the Styrofoam box housing an ECC ozonesonde.

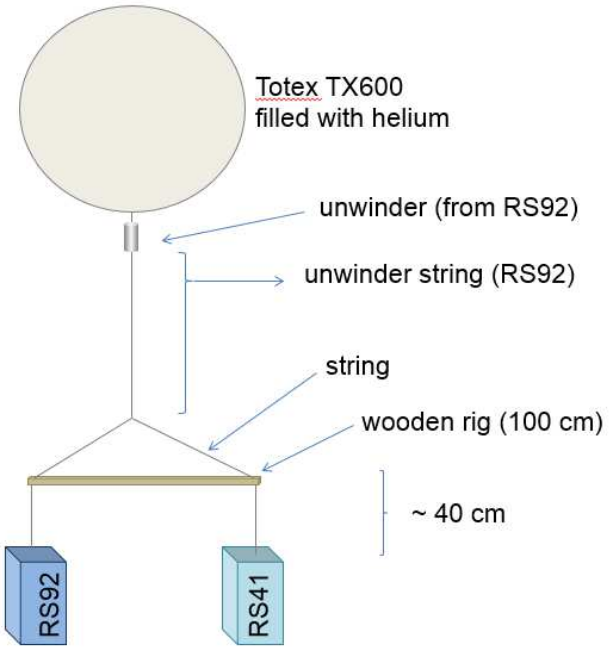

Figure 29: The rigging method for RS41-RS92 dual soundings used at Ny Ålesund between April 2016 and March 2018. Considering GRUAN Technical Note TN-7(*von Rohden et al.*, 2016), the strig between the wooden rig and the sondes has been lengthened to 70 cm after August 2016.

Figure 30: Photographs of a RS92-RS41 dual sounding at Ny Ålesund. The radiosnde eual soundings were performed in the framework of GRUAN, to provide simultaneous observations by the two radiosonde types, that allows for the detailed comparison and the identification of deviations.

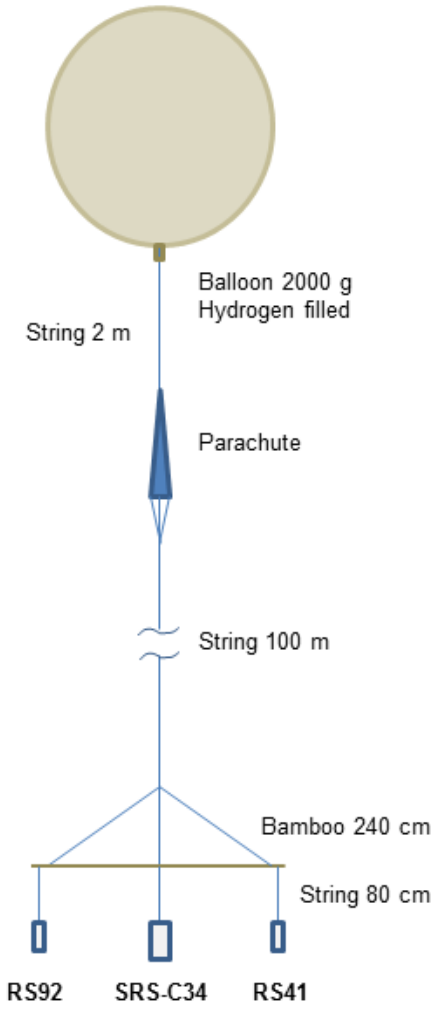

Figure 31: A schematic illustration of multiple payload with RS41, RS92, and Meteolabor SRS-C34 radiosonde used at Payerne, Switzerland.

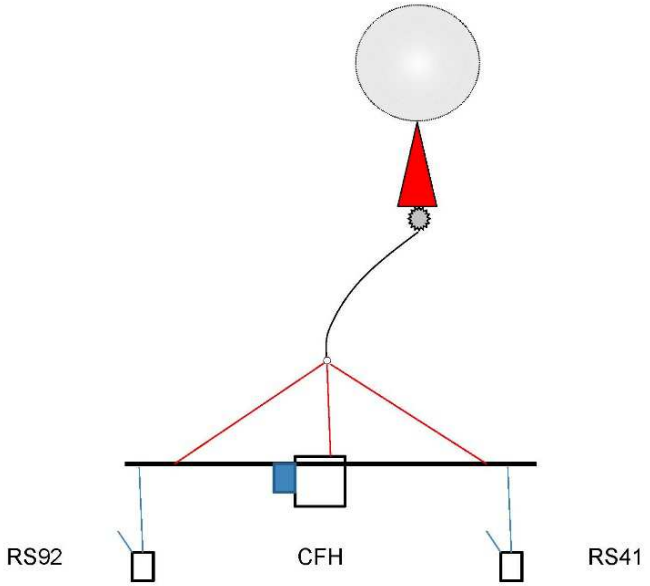

Figure 32: A typical CFH/RS41/RS92 payload configuration at Sodankylä, Finland. The payloads include CFH (with iMET1-RSB radiosonde and ECC ozonesonde) in the center. The boom is 2.5 m long and made of plastic. RS92 and RS41 radiosondes are hung at opposite ends of the boom using ∼80 cm-long strings cut from the Vaisala radiosondes unwinder. The payload also includes a parachute (TOTEX 160 cm), a Graw unwinder with a 60 m long string and typically a TOTEX T2000 balloon.

6 Summary and Discussion

In this document, we have reviewed various configurations of multiple-payload radiosonde soundings used at GRUAN and other sites. Multiple-payload soundings are necessary when the radiosonde type is changed at a GRUAN site to characterize the measurement uncertainty of both old and new instruments, thereby ensuring a homogeneous, long-term climate data record at the site. Multiple-payload soundings are also employed to measure profiles of ozone or particles, properties of particles, etc., in addition to the standard meteorological variables measured with an operational radiosonde. There are several variations in the multiple-payload rigging configurations whose components include balloon, parachute, unwinder, main string, booms, additional strings, and instruments. We have listed the physical effects influencing radiosonde measurements of temperature and relative humidity, and their influence on these measurements that each multiple-payload configuration may have. Great care needs to be taken in choosing the configuration, so that the data quality from multiple-payload soundings is minimally different from that for a single-payload flight. Ideally, the same method should be used throughout a network for a specific combination of payloads (e.g. RS41 and RS92) to minimize uncertainties arising from the use of different riggings. The ultimate goal is to make recommendations of specific configurations, with uncertainty estimation attached, for multiple-payload soundings at GRUAN and other sites. To do this we would need a large number of experimental multiple-payload soundings using different configurations at various locations, local times, and seasons, but currently this extensive set of data does not exist. Researchers in the field are encouraged to provide their multiple-payload results to the GRUAN Lead Centre (see https://www.gruan.org/). Thus, instead of making recommendations, we present the list of the necessary actions towards the best practice and recommendations on the multiple-payload configuration.
The following points should be considered when selecting multiple-payload methods:

1. Measurement biases caused by the payload configuration should be minimized.

2. The rigging-originated part of the measurement uncertainty should be at a level low enough to draw the conclusions about the instrument biases and uncertainties.

3. Launches should be made safely, following the International Civil Aviation Organization (ICAO) and national authorities regulations. Too complicated configurations should be avoided, so that launches are made successfully in various weather conditions (under strong surface-wind conditions, heavy rainfall, etc.).

We have discussed various physical effects that may have (or would theoretically have) influences on the measurements from multiple-payload soundings. Currently, however, not much information is available as to whether these have actual influences on the sounding data and how large the additional uncertainty is. This sets challenges to define detailed specifications for the boom and string materials, dimensions and instrument positioning, etc.
In practice, the following items need to be considered when determining recommended multiple-payload radiosonde sounding arrangements:

- Preferred rigging method(s) and related specific instructions
- Balloon types (e.g. materials) and sizes
- Boom dimensions and material
- Main string length

- Supporting strings arrangement, length
- Parachute and its location
- Unwinder
- How to combine other accessories (e.g. radar reflector) if necessary
- The Health and Safety aspects (risk assessment) when launching the payload under the range of environmental conditions expected.

Acknowledgements

We thank Michael Jensen for providing information about radiosonde intercomparison methods used in Atmospheric Radiation Measurement (ARM) Southern Great Plains facility site near Lamont, Oklahoma and Hironobu Yokota for providing information about the multi-payload launches at Tateno site, Japan. We are also grateful to Frank Schmidlin and Larry Miloshevich for their comments on an earlier version of the manuscript. We also like to thank Florian Schmidmer for providing information on unwinder technology used for high payloads.

References

Bodeker, G. E., S. Bojinski, D. Cimini, R. J. Dirksen, M. Haeffelin, J. W. Hannigan, D. F. Hurst, T. Leblanc, F. Madonna, M. Maturilli, A. C. Mikalsen, R. Philipona, T. Reale, D. J. Seidel, D. G. H. Tan, P. W. Thorne, H. Vömel, and J. Wang, Reference upper-air observations for climate: From concept to reality, *Bull. Amer. Meteor. Soc.*, **97**, 123–135, doi:10.1175/bams-d-14-00072.1, 2016.

CIMO, *Guide to Meteorological Instruments and Methods of Observation*, World Meteorological Organization, Geneva, 8th edition, 2014, URL `http://www.wmo.int/pages/prog/www/IMOP/CIMO-Guide.html`, [Accessed 9 January 2017].

Daniels, G. E., Measurement of Gas Temperature and the Radiation Compensating Thermocouple, *J. Appl. Meteor.*, **7**(6), 1026–1035, doi:10.1175/1520-0450(1968)007⟨1026:mogtat⟩2.0.co;2, 1968.

Dirksen, R. J., M. Sommer, F. J. Immler, D. F. Hurst, R. Kivi, and H. Vömel, Reference quality upper-air measurements: GRUAN data processing for the Vaisala RS92 radiosonde, *Atmos. Meas. Tech.*, **7**(12), 4463–4490, doi:10.5194/amt-7-4463-2014, 2014, URL `http://www.atmos-meas-tech.net/7/4463/2014/`.

Edwards, D., G. Anderson, T. Oakley, and P. Gault, Met Office Intercomparison of Vaisala RS92 and RS41 Radiosondes, Technical report, UKMO, 2014, URL `go.vaisala.com/gen4/downloads/Met_Office_Intercomparison_of_Vaisala_RS41_and_RS92_Radiosondes.pdf`.

Fujiwara, M., M. Shiotani, F. Hasebe, H. Vömel, S. J. Oltmans, P. W. Ruppert, T. Horinouchi, and T. Tsuda, Performance of the Meteolabor "Snow White" Chilled-Mirror Hygrometer in the Tropical Troposphere: Comparisons with the Vaisala RS80 A/H-Humicap Sensors, *J. Atmos. Ocean. Technol.*, **20**(11), 1534–1542, doi:10.1175/1520-0426(2003)020$⟨$1534:potmsw$⟩$2.0.co;2, 2003.

GCOS, Report of the third gcos reference upper air network implementation and coordination meeting (gruan icm-3), Technical Report GCOS-149, WMO-TD-No. 1575, 2011.

GCOS, The GCOS reference upper air network (GRUAN) Guide, Technical Report 171, WMO/WIGOS Technical Report 2013-03, 2013, URL http://www.wmo.int/pages/prog/gcos/Publications/gcos-171.pdf, [Accessed 8 April 2016].

Hurst, D. F., S. J. Oltmans, H. Vömel, K. H. Rosenlof, S. M. Davis, E. A. Ray, E. G. Hall, and A. F. Jordan, Stratospheric water vapor trends over Boulder, Colorado: Analysis of the 30 year Boulder record, *J. of Geophys. Res. Atmos.*, **116**(D2), D02,306, doi:10.1029/2010jd015065, 2011.

Immler, F. J., J. Dykema, T. Gardiner, D. N. Whiteman, P. W. Thorne, and H. Vömel, Reference Quality Upper-Air Measurements: guidance for developing GRUAN data products, *Atmos. Meas. Tech.*, **3**(5), 1217–1231, doi:10.5194/amt-3-1217-2010, 2010, URL http://www.atmos-meas-tech.net/3/1217/2010/.

Jeannet, P., C. Bower, and B. Calpini, Global criteria for tracing the improvements of radiosondes over the last decades, Technical Report 95, WMO/TD-No. 1433, Geneva, Switzerland, 2008.

Jensen, M. P., D. J. Holdridge, P. Survo, R. Lehtinen, S. Baxter, T. Toto, and K. L. Johnson, Comparison of Vaisala radiosondes RS41 and RS92 at the ARM Southern Great Plains site, *Atmos. Meas. Tech.*, **9**(7), 3115–3129, doi:10.5194/amt-9-3115-2016, 2016, URL http://www.atmos-meas-tech.net/9/3115/2016/.

Jumper, G., E. Murphy, and P. Tracy, Simultaneous balloon launches to investigate wake effects on thermosonde results, volume AIAA 2003-3605 (2003), doi:10.2514/6.2003-3605.

Kobayashi, E., Y. Noto, S. Wakino, H. Yoshii, T. Ohyoshi, S. Saito, and Y. Baba, Comparison of Meisei RS2-91 Rawinsondes and Vaisala RS92-SGP Radiosondes at Tateno for the Data Continuity for Climatic Data Analysis, *Journal of the Meteorological Society of Japan. Ser. II*, **90**(6), 923–945, doi:10.2151/jmsj.2012-605, 2012.

Kräuchi, A., R. Philipona, G. Romanens, D. F. Hurst, E. G. Hall, and A. F. Jordan, Controlled weather balloon ascents and descents for atmospheric research and climate monitoring, *Atmos. Meas. Tech.*, **9**(3), 929–938, doi:10.5194/amt-9-929-2016, 2016, URL http://www.atmos-meas-tech.net/9/929/2016/.

Luers, J. K., Estimating the temperature error of the radiosonde rod thermistor under different environments, *J. Atmos. Ocean. Technol.*, **7**, 882–895, doi:10.1175/1520-0426(1990)007⟨0882, 1990.

Luers, J. K. and R. E. Eskridge, Use of radiosonde temperature data in climate studies, *Int. J. Climatol.*, **11**, 10021019, 1998.

Mather, J. H. and J. W. Voyles, The Arm Climate Research Facility: A Review of Structure and Capabilities, *Bull. Amer. Meteor. Soc.*, **94**(3), 377–392, doi:10.1175/BAMS-D-11-00218.1, 2013, URL https://doi.org/10.1175/BAMS-D-11-00218.1.

McMillin, L., M. Uddstrom, and A. Coletti, A procedure for correcting radiosonde reports for radiation errors, *J. Atmos. Ocean. Technol.*, **9**, 801811, 1992.

Nash, J., Measurement of upper-air pressure, temperature and humidity, Technical Report 121, 2015.

Nash, J., T. Oakley, H. Vömel, and L. Wei, WMO Intercomparison of High Quality Radiosonde Systems Yangjiang, China, 12 July – 3 August 2010, Technical report, WMO, 2011, URL https://www.wmo.int/pages/prog/www/IMOP/publications/IOM-107%_Yangjiang/IOM-107_Yangjiang.zip, WMO/TD-No. 1580, Instruments And Observing Methods Report No. 107.

Nash, J., R. Smout, T. Oakley, B. Pathack, and S. Kurnosenko, WMO Intercomparison of Radiosonde Systems, Vacoas, Mauritius, 225 February 2005, Technical report, WMO, 2006, URL http://www.wmo.int/pmd_ged/wmo-td_1303_en.pdf, WMO/TD-No. 1303.

Philipona, R., A. Kräuchi, G. Romanens, G. Levrat, R. Ruppert, E. Brocard, P. Jeannet, D. Ruffieux, and B. Calpini, Solar and thermal radiation errors on upper-air radiosonde temperature measurements, *J. Atmos. Ocean. Technol.*, **30**, 2382–2393, doi:10.1175/JTECH-D-13-00047.1, 2013.

Schmidlin, F., J. K. Luers, and P. D. Huffman, Preliminary estimates of radiosonde thermistor errors, Technical report, 1986.

Seidel, D. J., F. H. Berger, F. Immler, M. Sommer, H. Vömel, H. J. Diamond, J. Dykema, D. Goodrich, W. Murray, T. Peterson, D. Sisterson, P. Thorne, and J. Wang, Reference upper-air observations for climate: Rationale, progress, and plans, *Bull. Amer. Meteor. Soc.*, **90**(3), 361–369, doi:10.1175/2008bams2540.1, 2009.

Shimizu, K. and F. Hasebe, Fast-response high-resolution temperature sonde aimed at contamination-free profile observations, *Atmos. Meas. Tech.*, **3**(6), 1673–1681, doi:10.5194/amt-3-1673-2010, 2010.

da Silveira, R. B., G. Fisch, L. A. T. Machado, A. DallAntonia Jr., L. F. Sapucci, D. Fernandes, and J. Nash, Executive Summary of the WMO Intercomparison of GPS Radiosondes (Brazil, 20 May to 10 June 2001), Technical Report 76, WMO/TD No. 1153, 2003.

Tiefenau, H. K. E. and A. Gebbeken, Influence of meteorological balloons on temperature measurements with radiosondes: Nighttime cooling and daylight heating, *J. Atmos. Ocean. Technol.*, **6**(1), 36–42, doi:10.1175/1520-0426(1989)006⟨0036:iombot⟩2.0.co;2, 1989.

Verver, G., M. Fujiwara, P. Dolmans, C. Becker, P. Fortuin, and L. Miloshevich, Performance of the Vaisala RS80 A/H and RS90 Humicap sensors and the Meteolabor Snow White chilled-mirror hygrometer in Paramaribo, Suriname, *J. Atmos. Ocean. Technol.*, **23**, 1506–1518, doi:10.1175/JTECH1941.1, 2006.

Vömel, H., D. E. David, and K. Smith, Accuracy of tropospheric and stratospheric water vapor measurements by the cryogenic frost point hygrometer: Instrumental details and observations, *J. of Geophys. Res. Atmos.*, **112**(D8), D08,305, doi:10.1029/2006jd007224, 2007a.

Vömel, H., H. Selkirk, L. Miloshevich, J. Valverde-Canossa, J. Valdés, E. Kyrö, R. Kivi, W. Stolz, G. Peng, and J. A. Diaz, Radiation Dry Bias of the Vaisala RS92 Humidity Sensor, *J. Atmos. Ocean. Technol.*, **24**(6), 953–963, doi:10.1175/jtech2019.1, 2007b.

Vömel, H., V. Yushkov, S. Khaykin, L. Korshunov, E. Kyrö, and R. Kivi, Intercomparisons of Stratospheric Water Vapor Sensors: FLASH-B and NOAA/CMDL Frost-Point Hygrometer, *J. Atmos. Ocean. Technol.*, **24**(6), 941–952, doi:10.1175/jtech2007.1, 2007c.

von Rohden, C., M. Sommer, and R. Dirksen, GRUAN Technical Note 7 - Rigging recommendations for dual radiosonde soundings, Technical report, GRUAN Lead Centre, Lindenberg, 2016, URL https://www.gruan.org/gruan/editor/documents/gruan/GRUAN-TN-7_Comparison_setup_v1.0_final.pdf, version 1.0.

Yagi, S., A. Mita, and N. Inoue, WMO international radiosonde comparison Phase IV Tsukuba, Japan, 15 February-12 March 1993 Final report, Technical Report 59, WMO/TD-No. 742, 1996, URL http://www.wmo.int/pmd_ged/wmo-td_742_en.pdf.